Appl Nanosci (2014) 4:511–521
DOI 10.1007/s13204-013-0234-9

REVIEW ARTICLE

Investigation of peristaltic flow of Williamson nanofluid in a curved channel with compliant walls

S. Nadeem · E. N. Maraj · Noreen Sher Akbar

Received: 19 April 2013 / Accepted: 11 May 2013 / Published online: 1 June 2013

Abstract In the present paper, we have examined the peristaltic flow of Williamson nanofluid in a curved channel comprising compliant walls. The governing equations of a Williamson fluid model with nanoparticles for curved channel are derived, including the effects of curvature and heat dissipation. The highly nonlinear, partial differential equations are simplified by using the wave frame transformation, long wave length and low Reynolds number assumptions. The reduced, nonlinear, coupled differential equations are solved analytically with the help of the homotopy perturbation method. The physical features of pertinent parameters have been discussed by plotting the graphs of velocity, temperature, concentration profile and stream functions.

Keywords Peristaltic flow · Williamson fluid · Nanoparticles · Curved channel · Compliant walls · Homotopy perturbation method

List of symbols

$\overline{N}$	Coordinate in cross-stream
$\overline{S}$	Coordinate in downstream
$\overline{Z}$	Coordinate in vertical direction
$\overline{V}$	Fluid velocity cross-stream component
$\overline{U}$	Fluid velocity downstream component
R^*	Radius of curvature
λ	Wave length
c	Wave speed
b	Wave amplitude
Re	Reynolds number
ρ_f	Fluid density
μ	Dynamic viscosity
$(\rho c)_f$	Heat capacity of the fluid
$(\rho c)_p$	Effective heat capacity of the nanoparticle material
κ	Thermal conductivity
D_B	Brownian diffusion coefficient
D_T	Thermophoretic diffusion coefficient
σ	Longitudinal tension per unit width
m	Mass per unit area
C	Coefficient of viscous damping
δ	Wave number
k	Curvature parameter
N_b	Brownian motion parameter
N_t	Thermophoresis parameter
G_r	Local temperature Grash of number
B_r	Local nanoparticle Grash of number

S. Nadeem · E. N. Maraj
Department of Mathematics, Quaid-i-Azam University, Islamabad, Pakistan

E. N. Maraj (✉) · N. S. Akbar
DBS & H, CEME, National University of Sciences and Technology, Islamabad, Pakistan
e-mail: ehnber@gmail.com

Introduction

Radially regular reduction and recreation of muscles which propagates in a wave down the muscular hose, in an interrogate way is known as peristalsis. In the human body, peristalsis originates with the contraction of smooth muscles to push inside through the digestive swathe. Earthworms use a similar mechanism to drive their locomotion. Peristaltic movement is initiated by circular smooth muscles contracting behind the chewed material to prevent it from moving back into the mouth. Peristalsis was first studied by Latham (1966) in 1965. He analyzed the fluid motion in a peristaltic pump. Recent literature regarding the peristaltic flow for Newtonian and non-Newtonian fluid can be found in Sato et al. (2000),

Mekheimer (2003), Mekheimer and Abd elmaboud (2008), Tripathi et al. (2010), Srinivas and Gayathri (2009), Nadeem and Akram (2010) and Akbar and Nadeem (2012a).

The idea of Kramer (1960) for compliant wall is extended by Mittra and Prasad (1973) for peristaltic flow. He discussed the peristaltic flow in a two-dimensional channel. They have projected vibrant boundary conditions to reflect on the stretchy/viscoelastic character of flexible boundaries and deliberate the forceful interaction of fluid and flexible walls which is intrinsic in peristalsis. Radhakrishnamacharya and Srinivasulu (1999) presented the problem of Mittra and Prasad (1973) under the long wavelength and low Reynolds number approximation. Muthu et al. (2001) described their study to axisymmetric tube for small values of amplitude ratio using the usual perturbation method. In another article, Muthu et al. (2003) extended the same work for micropolar fluid. They analyzed that for non-zero viscous damping, flow reversal is found at the wall of the flexible tube. The influence of wall properties on peristaltic transport with heat transfer is presented by Radhakrishnamacharya and Srinivasulu (2007). They found that heat transfer increases with elastic tension and mass characterizing parameters. Some other articles are cited by Srinivas et al. (2009), Srinivas and Kothandapani (2009), Afifi et al. (2011) and Rathod and Pallavi (2011).

A nanofluid is an auxiliary or less consistent diffusion of unyielding particles among tiny diameters deliberate in nanometers. These particles are balanced by Brownian motions and when they are in symmetry with no flow they are dispersed in a balance between optimistic mass plus thermal campaigning (Brownian motions). The awareness of nanofluid has been vastly urbanized by Choi (1995). The problem of laminar forced convection flow of nanofluids has been thoroughly investigated by Marga et al. (2005) for two particular geometrical configurations, namely, a uniformly heated tube and a system of parallel coaxial and heated disks. Heat transfer enhancement utilizing nanofluids in a trapezoidal enclosure is investigated by Saleh et al. (2011) for various pertinent parameters. They modelled transport equations by a stream-vorticity formulation and solved numerically by finite difference approach. An endoscopic effect on the peristaltic flow of a nanofluid is discussed by Akbar and Nadeem (2011). They analyzed the problem between two concentric tubes and also discussed the properties of the endoscope. Subsequent investigations conducted on nanofluids are cited by Aziz and Khan (2012), Nadeem and Maraj (2012) and Akbar and Nadeem (2012b).

To the best of our knowledge, investigation of nano-Williamson fluid in a curved channel has not been undertaken yet. Therefore, the purpose of the present paper is to analyze the peristaltic flow of a nanoWilliamson fluid in a curved channel. The flow fields, temperature distributions, nanoparticle phenomena and streamlines have been calculated using homotopy perturbation technique and are presented graphically.

Mathematical formulation

Consider a two-dimensional flow of an incompressible Williamson nanofluid in a curved channel of uniform thickness $2a$. The channel walls are flexible and compliant on which small amplitudes of the travelling waves are imposed. Define $(\overline{N},\overline{S},\overline{Z})$ as the coordinates in the cross-stream, downstream and vertical directions, respectively, and R^* as the radius of curvature. The flow in the channel is induced by sinusoidal waves of small amplitude b travelling along the flexible walls of the channel. The walls of the channel are considered as follows:

$$\overline{N} = H(\overline{S},\overline{t}) = a + b\sin\left[\frac{2\pi}{\lambda}(\overline{S} - c\overline{t})\right], \quad \text{upper wall} \tag{1}$$

$$\overline{N} = -H(\overline{S},\overline{t}) = -a - b\sin\left[\frac{2\pi}{\lambda}(\overline{S} - c\overline{t})\right], \quad \text{lower wall} \tag{2}$$

In the above equations c is the wave speed and λ denotes the wave length. Let $\overline{V}$ and $\overline{U}$ denote the velocity components in the cross-stream and downstream directions, respectively. The governing equations for motion, energy and nanoparticle for curved channel are described as:

$$\frac{R^*}{\overline{N}+R^*}\frac{\partial}{\partial\overline{N}}\left(\frac{(\overline{N}+R^*)}{R^*}\overline{V}\right) + \frac{R^*}{\overline{N}+R^*}\frac{\partial\overline{U}}{\partial\overline{S}} = 0, \tag{3}$$

$$\rho_{\mathrm{f}}\left(\frac{\partial\overline{V}}{\partial\overline{t}} + \overline{V}\frac{\partial\overline{V}}{\partial\overline{N}} + \frac{R^*\overline{U}}{\overline{N}+R^*}\frac{\partial\overline{V}}{\partial\overline{S}} - \frac{\overline{U}^2}{\overline{N}+R^*}\right) = -\frac{\partial\overline{P}}{\partial\overline{N}} + \frac{\partial}{\partial\overline{N}}(\overline{\tau}_{\overline{NN}}) + \frac{R^*}{\overline{N}+R^*}\frac{\partial}{\partial\overline{S}}(\overline{\tau}_{\overline{NS}}) - \frac{\overline{\tau}_{\overline{SS}}}{\overline{N}+R^*}, \tag{4}$$

$$\rho_{\mathrm{f}}\left(\frac{\partial\overline{U}}{\partial\overline{t}} + \overline{V}\frac{\partial\overline{U}}{\partial\overline{N}} + \frac{R^*\overline{U}}{\overline{N}+R^*}\frac{\partial\overline{U}}{\partial\overline{S}} + \frac{\overline{U}\overline{V}}{\overline{N}+R^*}\right) = -\frac{R^*}{\overline{N}+R^*}\frac{\partial\overline{P}}{\partial\overline{S}} + \frac{\partial}{\partial\overline{N}}(\overline{\tau}_{\overline{NS}}) + \frac{R^*}{\overline{N}+R^*}\frac{\partial}{\partial\overline{S}}(\overline{\tau}_{\overline{SS}}) + \rho g\alpha(\overline{T}-T_0) + \rho g\alpha(\overline{C}-C_0), \tag{5}$$

$$(\rho c)_{\mathrm{f}}\frac{\mathrm{d}\overline{T}}{\mathrm{d}\overline{t}} = \kappa\nabla^2\overline{T} + (\rho c)_{\mathrm{p}}\left[D_{\mathrm{B}}\nabla\overline{C}\cdot\nabla\overline{T} + \frac{D_{\mathrm{T}}}{T_0}\nabla\overline{T}\cdot\nabla\overline{T}\right] + \overline{\boldsymbol{\tau}}\cdot\overline{L}, \tag{6}$$

$$\frac{\mathrm{d}\overline{C}}{\mathrm{d}\overline{t}} = D_{\mathrm{B}}\nabla^2\overline{C} + \frac{D_{\mathrm{T}}}{T_0}\nabla^2\overline{T}. \tag{7}$$

In the above equations, $\overline{P}$ is the pressure, $\overline{V}$ and $\overline{U}$ are the velocity components in cross-stream $\overline{N}$ and downstream $\overline{S}$ directions, respectively; R^* is constant radius and $\overline{\tau}$'s represent the stresses which are defined as:

$$\tau_{\overline{NN}} = 2\eta_0\left[1 + \Gamma|\dot{\overline{\gamma}}|\right]\frac{\partial\overline{V}}{\partial\overline{N}}, \tag{8}$$

$$\tau_{\overline{SN}} = \tau_{\overline{NS}} = \eta_0\left[1+\Gamma\left|\dot{\overline{\gamma}}\right|\right]\left(\frac{\partial \overline{U}}{\partial \overline{N}} + \frac{R^*}{\overline{N}+R^*}\frac{\partial \overline{V}}{\partial \overline{S}} - \frac{\overline{U}}{\overline{N}+R^*}\right), \tag{9}$$

$$\tau_{\overline{SS}} = 2\eta_0\left[1+\Gamma\left|\dot{\overline{\gamma}}\right|\right]\left(\frac{R^*}{\overline{N}+R^*}\frac{\partial \overline{U}}{\partial \overline{S}} + \frac{\overline{V}}{\overline{N}+R^*}\right). \tag{10}$$

The corresponding boundary conditions for asymmetric channel having compliant walls are defined as:

$$\overline{U} = 0 \text{ at } \overline{N} = \pm H = \pm\left[a + b\sin\left(\frac{2\pi}{\lambda}(\overline{S} - c\overline{t})\right)\right], \tag{11}$$

$$\frac{R^*}{\overline{N}+R^*}\frac{\partial}{\partial \overline{S}}L(H) = \frac{R^*}{\overline{N}+R^*}\frac{\partial \overline{P}}{\partial \overline{S}} \quad \text{at } \overline{N} = \pm H, \tag{12}$$

$$\overline{T} = T_0, \quad \overline{C} = C_0 \quad \text{on } \overline{N} = -H, \tag{13}$$

$$\overline{T} = T_1, \quad \overline{C} = C_1 \quad \text{on } \overline{N} = H. \tag{14}$$

Here ρ_f, μ, $(\rho c)_f$, $(\rho c)_p$, κ, D_B and D_T are the fluid density, dynamic viscosity, heat capacity of the fluid, effective heat capacity of the nanoparticle material, thermal conductivity, Brownian diffusion coefficient and thermophoretic diffusion coefficient, respectively. Moreover,

$$L = B\frac{\partial^4}{\partial \overline{S}^4} - \sigma\frac{\partial^2}{\partial \overline{S}^2} + m\frac{\partial^2}{\partial t^2} + C\frac{\partial}{\partial t} + K, \tag{15}$$

where B is the flexural rigidity of the wall, σ is the longitudinal tension per unit width, m is the mass per unit area, C is the coefficient of viscous damping and K is spring stiffness.

The following non-dimensional variables and velocity stream function relationship are introduced:

$$s = \frac{\overline{S}}{\lambda}, \quad n = \frac{\overline{N}}{a}, \quad u = \frac{\overline{U}}{c}, \quad v = \frac{\overline{V}}{c},$$
$$\psi = \frac{\overline{\psi}}{ca}, \quad t = \frac{c\overline{t}}{\lambda}, \quad k = \frac{R^*}{a}, \quad Re = \frac{\rho_f c a}{\eta_0},$$
$$\varepsilon = \frac{b}{a}, \quad \alpha = \frac{\kappa}{(\rho c)_f},$$
$$\delta = \frac{a}{\lambda}, \quad p = \frac{a^2\overline{P}}{c\eta_0\lambda}, \quad \theta = \frac{\overline{T}-T_1}{T_0-T_1},$$
$$\sigma = \frac{\overline{C}-C_1}{C_0-C_1}, \quad G_r = \frac{g\alpha a^2(T_0-T_1)}{vc},$$
$$\beta 3 = \frac{\eta_0 c^2}{(T_1-T_0)\alpha(\rho c)_f},$$
$$E_4 = -\frac{\sigma a^3}{\lambda^3\eta_0 c}, \quad E_1 = \frac{mca^3}{\lambda^3\eta_0}, \quad E_2 = \frac{Ca^3}{\lambda^2\eta_0},$$
$$E_3 = \frac{Ba^3}{\eta_0 c\lambda^5}, \quad E_5 = \frac{Ka^3}{\eta_0 c\lambda}, \quad B_r = \frac{g\alpha a^2(C_0-C_1)}{vc},$$
$$N_b = \frac{(\rho c)_p D_B C_0}{\alpha(\rho c)_f}, \quad N_t = \frac{(\rho c)_p D_T T_0}{\alpha(\rho c)_f},$$
$$W_e = \frac{\Gamma a}{d}, \quad u = -\frac{\partial\psi}{\partial n}, \quad v = \delta\frac{k}{n+k}\frac{\partial\psi}{\partial s}.$$

Equation (3) is identically satisfied and Eqs. (4)–(11) under long wavelength and low Reynolds number approximations are expressed in the following dimensionless form:

$$\frac{\partial p}{\partial n} = 0, \tag{16}$$

$$\left(\frac{k}{n+k}\right)\frac{\partial p}{\partial s} = \frac{\partial}{\partial n}\left[\left(\frac{1}{n+k}\frac{\partial\psi}{\partial n} - \frac{\partial^2\psi}{\partial n^2}\right) + W_e\left(\frac{1}{n+k}\frac{\partial\psi}{\partial n} - \frac{\partial^2\psi}{\partial n^2}\right)^2\right] + G_r\theta + B_r\sigma, \tag{17}$$

$$\frac{\partial^2\theta}{\partial n^2} + \frac{1}{n+k}\frac{\partial\theta}{\partial n} + N_b\frac{\partial\sigma}{\partial n}\frac{\partial\theta}{\partial n} + N_t\left(\frac{\partial\theta}{\partial n}\right)^2 + \beta_3\left[\left(\frac{1}{n+k}\frac{\partial\psi}{\partial n} - \frac{\partial^2\psi}{\partial n^2}\right)^2 + W_e\left(\frac{1}{n+k}\frac{\partial\psi}{\partial n} - \frac{\partial^2\psi}{\partial n^2}\right)^3\right] = 0, \tag{18}$$

$$\frac{\partial}{\partial n}\left[(n+k)\frac{\partial\sigma}{\partial n}\right] + \frac{N_t}{N_b}\frac{\partial}{\partial n}\left[(n+k)\frac{\partial\theta}{\partial n}\right] = 0, \tag{19}$$

$$\frac{d\psi}{dn} = 0, \quad \frac{\partial^3\psi}{\partial n^3} = 0 \text{ at } n = \pm h = \pm[1+\varepsilon\sin 2\pi(s-t)], \tag{20}$$

$$\frac{\partial}{\partial n}\left[\left(\frac{1}{n+k}\frac{\partial\psi}{\partial n} - \frac{\partial^2\psi}{\partial n^2}\right) + W_e\left(\frac{1}{n+k}\frac{\partial\psi}{\partial n} - \frac{\partial^2\psi}{\partial n^2}\right)^2\right] + G_r\theta + B_r\sigma = \left[E_1\frac{\partial^3 h}{\partial t^2\partial s} + E_2\frac{\partial^2 h}{\partial t\partial s} + E_3\frac{\partial^5 h}{\partial s^5} + E_4\frac{\partial^3 h}{\partial s^3} + E_5\frac{\partial h}{\partial s}\right] \text{ at } n = \pm h, \tag{21}$$

$$\theta = 1, \quad \sigma = 1 \quad \text{at } n = -h, \tag{22}$$

$$\theta = 0, \quad \sigma = 0 \quad \text{at } n = h. \tag{23}$$

Solution of the problem

In order to solve the coupled nonlinear differential equations (17)–(19) with the help of HPM, we construct the following homotopic equations:

$$H(\psi,\tilde{p}) = (1-\tilde{p})\left[\frac{\partial}{\partial n}\left(\frac{1}{n+k}\frac{\partial\psi}{\partial n} - \frac{\partial^2\psi}{\partial n^2}\right) - \left(\frac{\partial}{\partial n}\left(\frac{1}{n+k}\frac{\partial\widetilde{\psi}_0}{\partial n} - \frac{\partial^2\widetilde{\psi}_0}{\partial n^2}\right)\right)\right] + \tilde{p}\left[\frac{\partial}{\partial n}\left\{\left(\frac{1}{n+k}\frac{\partial\psi}{\partial n} - \frac{\partial^2\psi}{\partial n^2}\right) + W_e\left(\frac{1}{n+k}\frac{\partial\psi}{\partial n} - \frac{\partial^2\psi}{\partial n^2}\right)^2\right\} + G_r\theta + B_r\sigma - \frac{k}{n+k}\frac{\partial}{\partial s}\left(E_1\frac{\partial^3 h}{\partial t^2\partial s} + E_2\frac{\partial^2 h}{\partial t^2} + E_3\frac{\partial^5 h}{\partial s^5} + E_4\frac{\partial^3 h}{\partial s^3} + E_5 h\right)\right] = 0, \tag{24}$$

$$H(\theta,\tilde{p}) = (1-\tilde{p})\left[\left(\frac{\partial^2\theta}{\partial n^2}+\frac{1}{(n+k)}\frac{\partial\theta}{\partial n}\right)-\left(\frac{\partial^2\tilde{\theta}_0}{\partial n^2}+\frac{1}{(n+k)}\frac{\partial\tilde{\theta}_0}{\partial n}\right)\right] + \tilde{p}\left[\frac{\partial^2\theta}{\partial n^2}+\frac{1}{(n+k)}\frac{\partial\theta}{\partial n}+\frac{1}{(n+k)}\frac{\partial\theta}{\partial n}+N_b\frac{\partial\sigma}{\partial n}\frac{\partial\theta}{\partial n}+N_t\left(\frac{\partial\theta}{\partial n}\right)^2 + \beta_3\left\{\left(\frac{1}{n+k}\frac{\partial\psi}{\partial n}-\frac{\partial^2\psi}{\partial n^2}\right)^2+W_e\left(\frac{1}{n+k}\frac{\partial\psi}{\partial n}-\frac{\partial^2\psi}{\partial n^2}\right)^3\right\}\right] = 0, \tag{25}$$

$$H(\sigma,\tilde{p}) = (1-\tilde{p})\left[\frac{\partial^2\sigma}{\partial n^2}+\frac{1}{(n+k)}\frac{\partial\sigma}{\partial n}-\left(\frac{\partial^2\tilde{\sigma}_0}{\partial n^2}+\frac{1}{(n+k)}\frac{\partial\tilde{\sigma}_0}{\partial n}\right)\right] + \tilde{p}\left[\frac{\partial^2\sigma}{\partial n^2}+\frac{1}{(n+k)}\frac{\partial\sigma}{\partial n}+\left\{\frac{N_t}{N_b}\frac{\partial^2\theta}{\partial n^2}+\frac{1}{n+k}\frac{\partial\theta}{\partial n}\right\}\right] = 0. \tag{26}$$

Using

$$\psi = \psi_0 + \tilde{p}\psi_1 + \tilde{p}^2\psi_2 + \cdots, \tag{27}$$

$$\theta = \theta_0 + \tilde{p}\theta_1 + \tilde{p}^2\theta_2 + \cdots, \tag{28}$$

$$\sigma = \sigma_0 + \tilde{p}\sigma_1 + \tilde{p}^2\sigma_2 + \cdots \tag{29}$$

Making use of Eqs. (27)–(29) into Eqs. (24)–(26) along with the boundary conditions (20) and (23), the solutions can be directly written as when $\tilde{p} \to 1$. The drawn out solutions are graphically discussed in the next section in detail.

Results and discussion

The effects of various patient parameters, i.e., curvature parameter k, W_e, N_b, N_t, B_r, G_r and heat dissipation parameter β_3 are graphically discussed for fluid velocity, temperature profile and concentration. The effect of various wall properties is displayed in Fig. 1. It is predicted that the

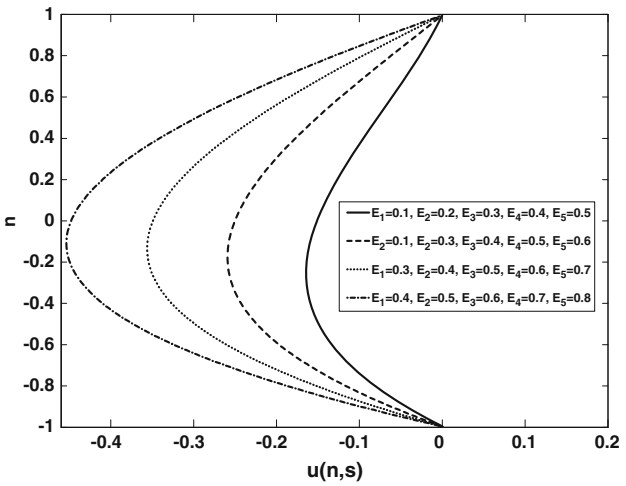

Fig. 1 Display the effect of wall properties of the compliant walls for different values of E_1, E_2, E_3, E_4, E_5 where $G_r = 0.5, B_r = 0.2, k = 2, s = 0.01, t = 0.05, \varepsilon = 0.1$ and $F = 2$

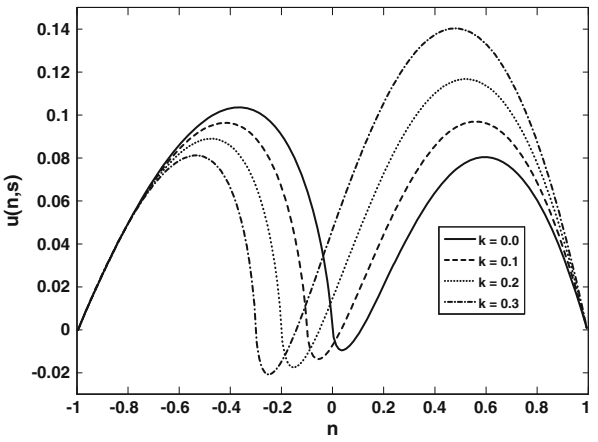

Fig. 2 The effect of k on velocity profile. Plots are shown for different values of k where $G_r = 0.5, B_r = 0.2, W_e = 0.01, s = 0.01, t = 0.05, \varepsilon = 0.1, E_1 = 0.1, E_2 = 0.5, E_3 = 0.1, E_4 = 0.5, E_5 = 0.1$ and $F = 2$

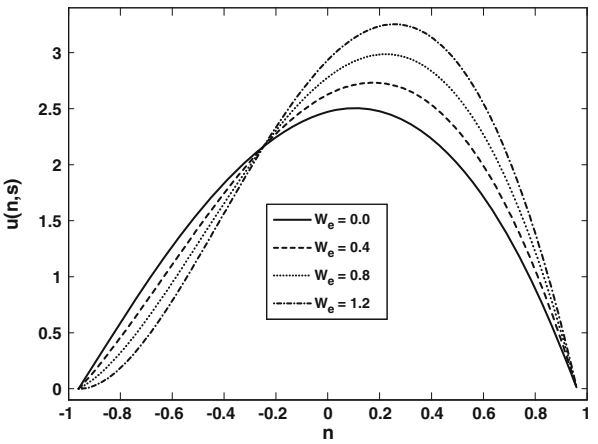

Fig. 3 Explains the behavior for different values of W_e where $G_r = 2, B_r = 3, k = 2, s = 0.1, t = 0.5, \varepsilon = 0.1, E_1 = 1, E_2 = 5, E_3 = 1, E_4 = 5, E_5 = 1$ and $F = 0.1$

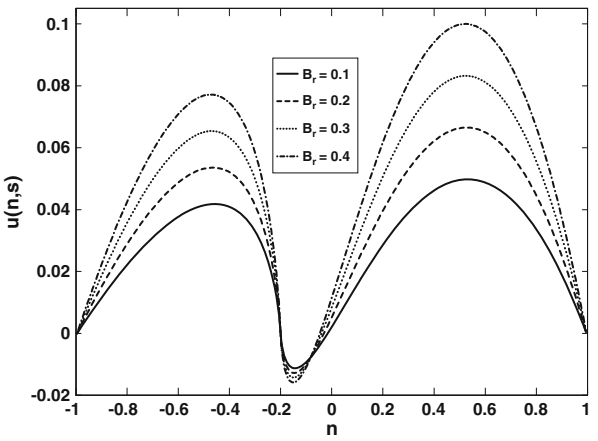

Fig. 4 Is a plot for velocity component $u(n,s)$ against n. It shows the effect of thermophoresis parameter B_r where $G_r = 0.2, k = 0.2, W_e = 0.01, s = 0.01, t = 0.5, \varepsilon = 0.1, E_1 = 0.1, E_2 = 0.5, E_3 = 0.1, E_4 = 0.5, E_5 = 0.1$ and $F = 2$

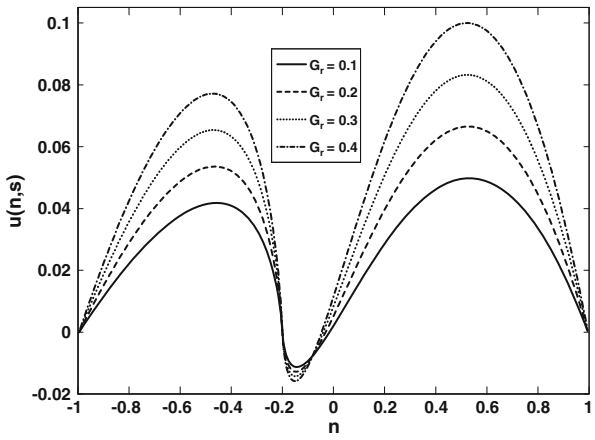

Fig. 5 The effect of G_r where $k = 0.2, B_r = 0.2, W_e = 0.01, s = 0.01, t = 0.05, \varepsilon = 0.1, E_1 = 0.1, E_2 = 0.5, E_3 = 0.1, E_4 = 0.5, E_5 = 0.1$ and $F = 2$

fluid velocity increases with enhancing wall properties. Figures 2, 3, 4 and 5 are plotted to illustrate the effects of patient parameters on velocity field. In Fig. 2, the effects of curvature parameter k are studied. It is observed that in the inner half of the channel the increase in curve-ness contributes in reducing fluid velocity. However, in the outer half of the channel more curve-ness allows fluid to flow more freely, i.e., the fluid velocity increases. Figure 3 displays the influence of fluid property W_e. We note that the velocity increases with the increase in W_e in the region close to the inner wall $[-1, -0.2]$ and decreases in the region close to the outer wall of the curved channel. Figure 4 displays the graphs for different values of B_r. It is noticed that with a raise in B_r, velocity increases. Moreover, it is seen that in the region close to the inner wall this increase is lessened as compared to the increase in the region close to the outer wall of the channel. Figure 5 displays the graphs for different values of G_r, the increase

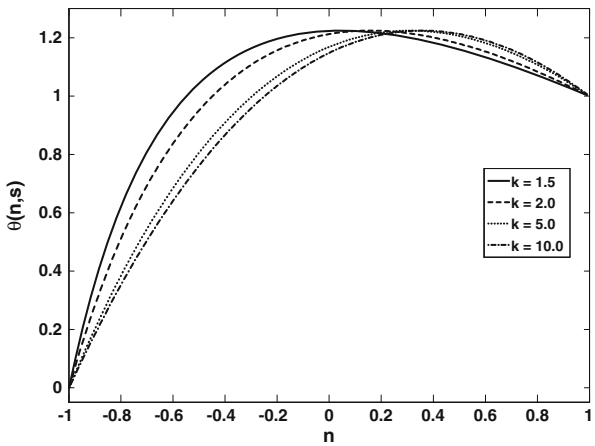

Fig. 6 The effect of k where $N_b = 2, N_t = 3, \beta_3 = 0.1, W_e = 0.01, s = 0.01, t = 0.05, \varepsilon = 0.1, E_1 = 0.1, E_2 = 0.5, E_3 = 0.1, E_4 = 0.5, E_5 = 0.1$ and $F = 2$

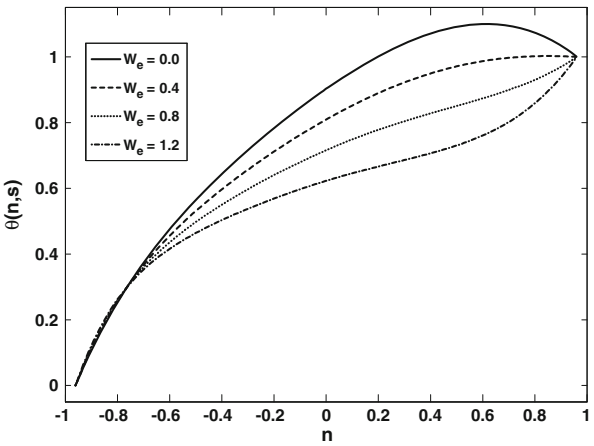

Fig. 7 Is a plot for temperature $\theta(n, s)$ against n. It shows the effects for different values of W_e where $N_b = 0.1, N_t = 0.3, \beta_3 = 0.5, k = 2, s = 0.1, t = 0.5, \varepsilon = 0.1, E_1 = 1, E_2 = 5, E_3 = 1, E_4 = 5, E_5 = 1$ and $F = 0.1$

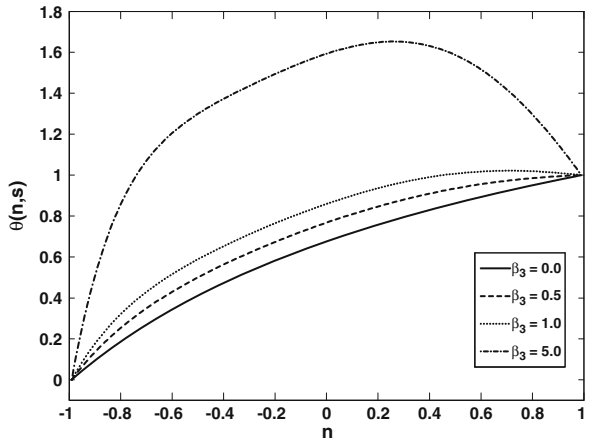

Fig. 8 The effect of β_3 where $N_b = 0.1, N_t = 0.3, k = 2, W_e = 0.5, s = 0.1, t = 0.5, \varepsilon = 0.1, E_1 = 1, E_2 = 5, E_3 = 1, E_4 = 5, E_5 = 1$ and $F = 0.1$

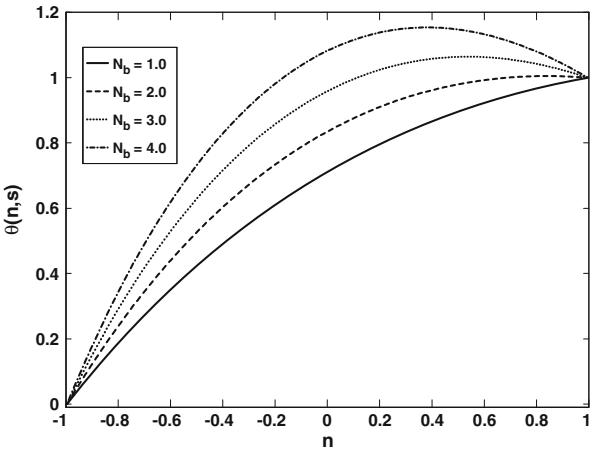

Fig. 9 The effect of N_b where $k = 5, N_t = 0.3, \beta_3 = 0.1, W_e = 0.01, s = 0.01, t = 0.05, \varepsilon = 0.1, E_1 = 0.1, E_2 = 0.5, E_3 = 0.1, E_4 = 0.5, E_5 = 0.1$ and $F = 2$

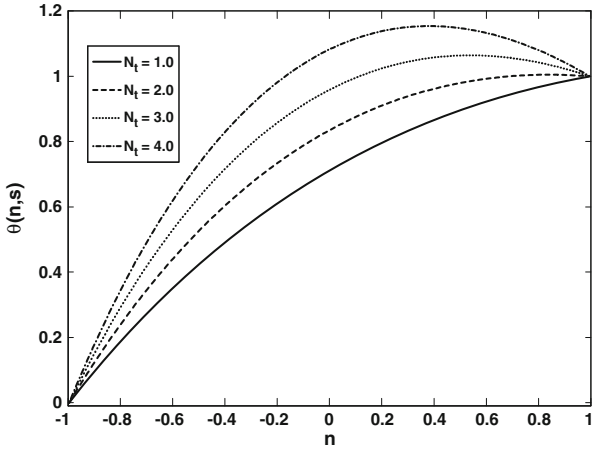

Fig. 10 Is plot for $\theta(n, s)$ against n. It shows the effect of N_{t} where $k = 5, N_{\mathrm{b}} = 0.3, \beta_3 = 0.1, W_{\mathrm{e}} = 0.01, s = 0.01, t = 0.05, \varepsilon = 0.1, E_1 = 0.1, E_2 = 0.5, E_3 = 0.1, E_4 = 0.5, E_5 = 0.1$ and $F = 2$

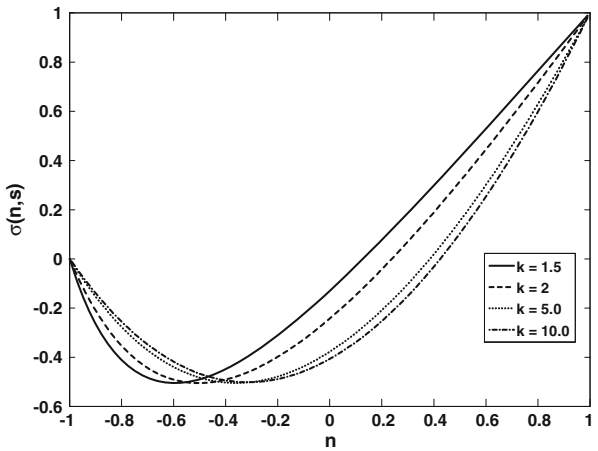

Fig. 11 Is the plot for $\sigma(n, s)$ against n. It shows the effect of k where $N_{\mathrm{b}} = 2, N_{\mathrm{t}} = 3, \beta_3 = 0.1, W_{\mathrm{e}} = 0.01, s = 0.01, t = 0.05, \varepsilon = 0.01, E_1 = 0.1, E_2 = 0.5, E_3 = 0.1, E_4 = 0.5, E_5 = 0.1$ and $F = 2$

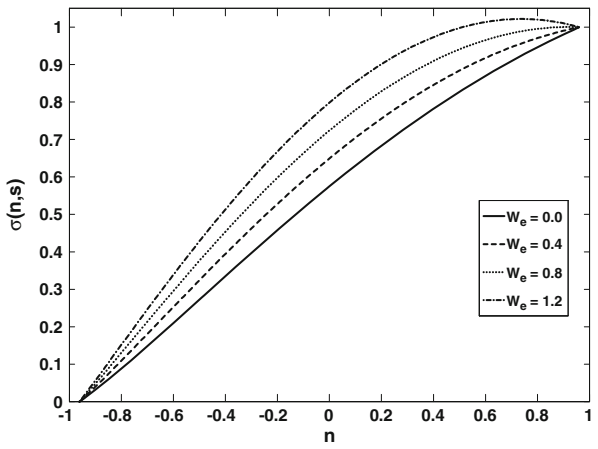

Fig. 12 The effect of W_{e} where $N_{\mathrm{b}} = 0.1, N_{\mathrm{t}} = 0.3, \beta_3 = 0.5, k = 2, s = 0.1, t = 0.5, \varepsilon = 0.1, E_1 = 0.1, E_2 = 0.5, E_3 = 0.1, E_4 = 0.5,\ E_5 = 0.1$ and $F = 0.1$

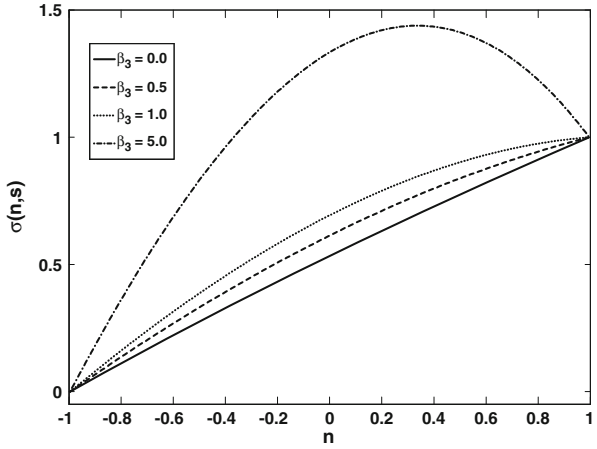

Fig. 13 The effect of β_3 where $N_{\mathrm{b}} = 0.3, N_{\mathrm{t}} = 0.1, k = 5, W_{\mathrm{e}} = 0.01, s = 0.01, t = 0.05, \varepsilon = 0.1, E_1 = 0.1, E_2 = 0.5, E_3 = 0.1, E_4 = 0.5, E_5 = 0.1$ and $F = 2$

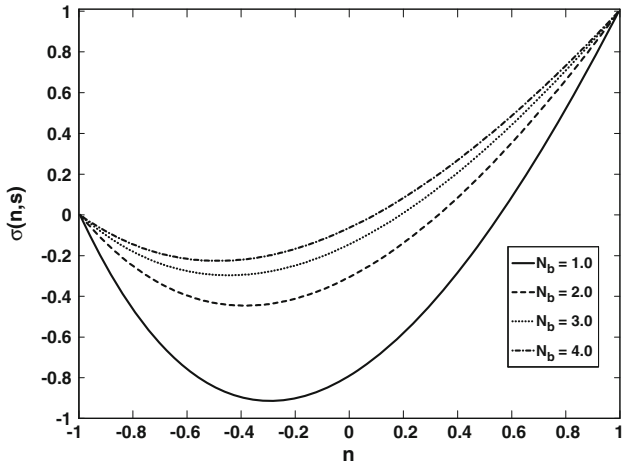

Fig. 14 The effect of N_{b} where $k = 5, N_{\mathrm{t}} = 3, \beta_3 = 0.1, W_{\mathrm{e}} = 0.01, s = 0.01, t = 0.05, \varepsilon = 0.01, E_1 = 0.1, E_2 = 0.5, E_3 = 0.1, E_4 = 0.5, E_5 = 0.1$ and $F = 2$

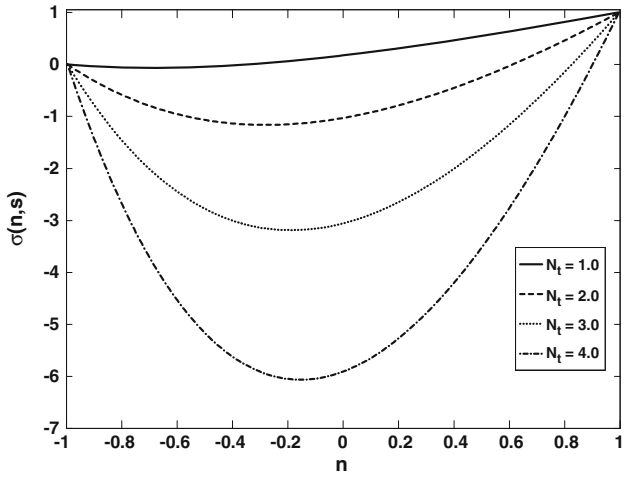

Fig. 15 The effect of N_{t} where $N_{\mathrm{b}} = 0.3, k = 5, \beta_3 = 0.1, W_{\mathrm{e}} = 0.01, s = 0.01, t = 0.05, \varepsilon = 0.01, E_1 = 0.1, E_2 = 0.5, E_3 = 0.1, E_4 = 0.5, E_5 = 0.1$ and $F = 2$

in G_r contribution in enhancing the fluid velocity. Figures 6, 7, 8, 9 and 10 are graphs for temperature profile θ against n for different values of k, W_e, β_3, N_b and N_t. In Fig. 6, the effect of k is discussed. It is observed that an increase in curvature parameter reduces temperature in the lower half of the channel while it contributes in raising temperature in the upper half of the channel. Fluid property parameter W_e effect is shown in Fig. 7. Notably temperature trim downs with taking into account large values of W_e. Figure 8 shows the effect of β_3. Note that β_3 shows the contribution of heat dissipation. We note an increase in θ with an increase in β_3 within the curved channel. Figure 9 is a graph for different values of N_b, which shows increase in θ with the increase in N_b. In Fig. 10 the effect of N_t is illustrated, increase in N_t increases θ. Figures 11, 12, 13, 14 and 15 are the plots for concentration σ against n. Figure 11 shows the role of curvature parameter k, we note that σ increases with the increase in k near the inner wall of the channel but it decreases in the region beyond inner wall to the outer wall region. The effect of fluid property is shown in Fig. 12. Notably the concentration increases by taking into account the large value of W_e. In Fig. 13 the effect of β_3 is shown on concentration. We note an increase in concentration with an increase in β_3. Figure 14 shows the behavior of σ for different values of N_b. It is observed that with increase in N_b, σ increases. Figure 15 shows the effect of N_t on σ. From Fig. 15 we conclude that σ decreases with an increase in N_t. Figures 16, 17, 18 and 19 are the streamlines plotted for different values of pertinent parameters. In Fig. 16 streamlines are plotted for different

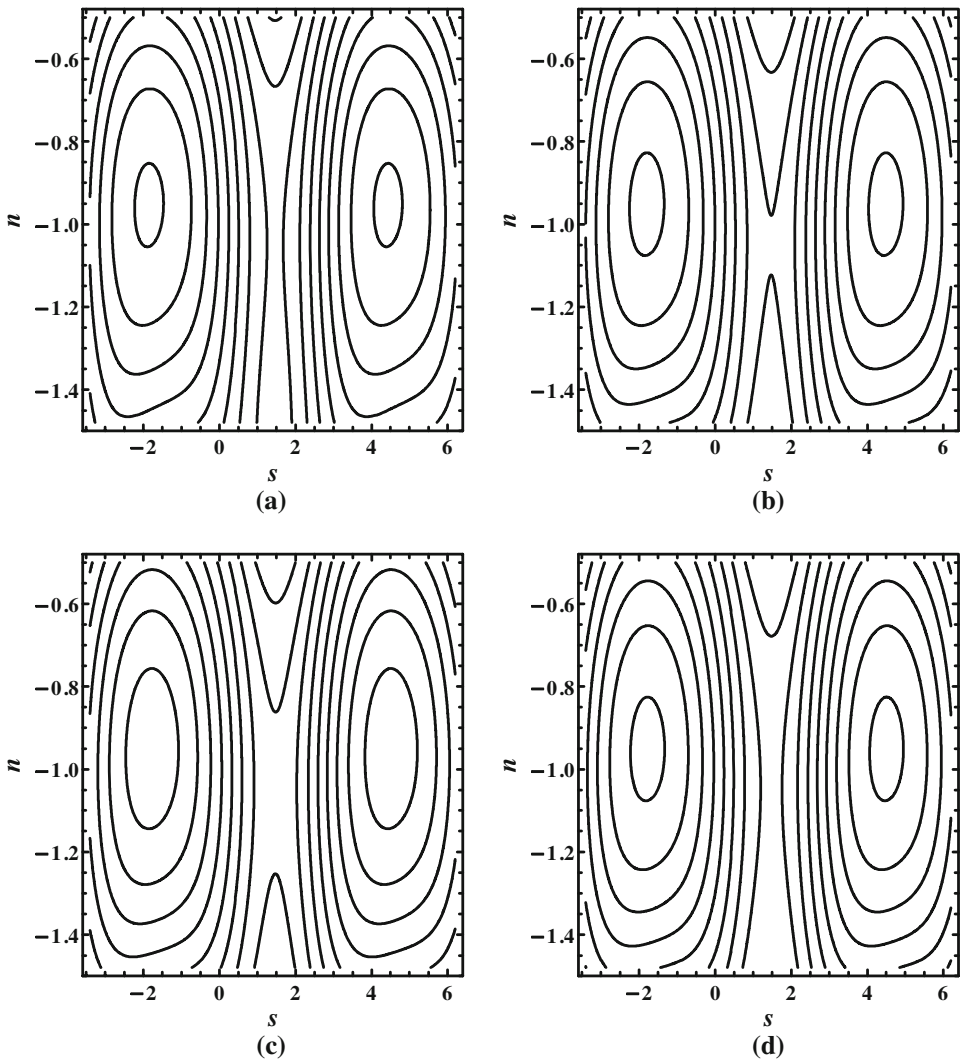

Fig. 16 Here the streamlines are plotted for against different values of k, i.e. **a** $k = 2$, **b** $k = 5$, **c** $k = 10$, **d** $k = 20$ while $B_r = 0.1, G_r = 0.2, W_e = 0.1, t = 0.05, \varepsilon = 0.05, E_1 = 0.1, E_2 = 0.5, E_3 = 0.1, E_4 = 0.5, E_5 = 0.1$ and $F = 2$

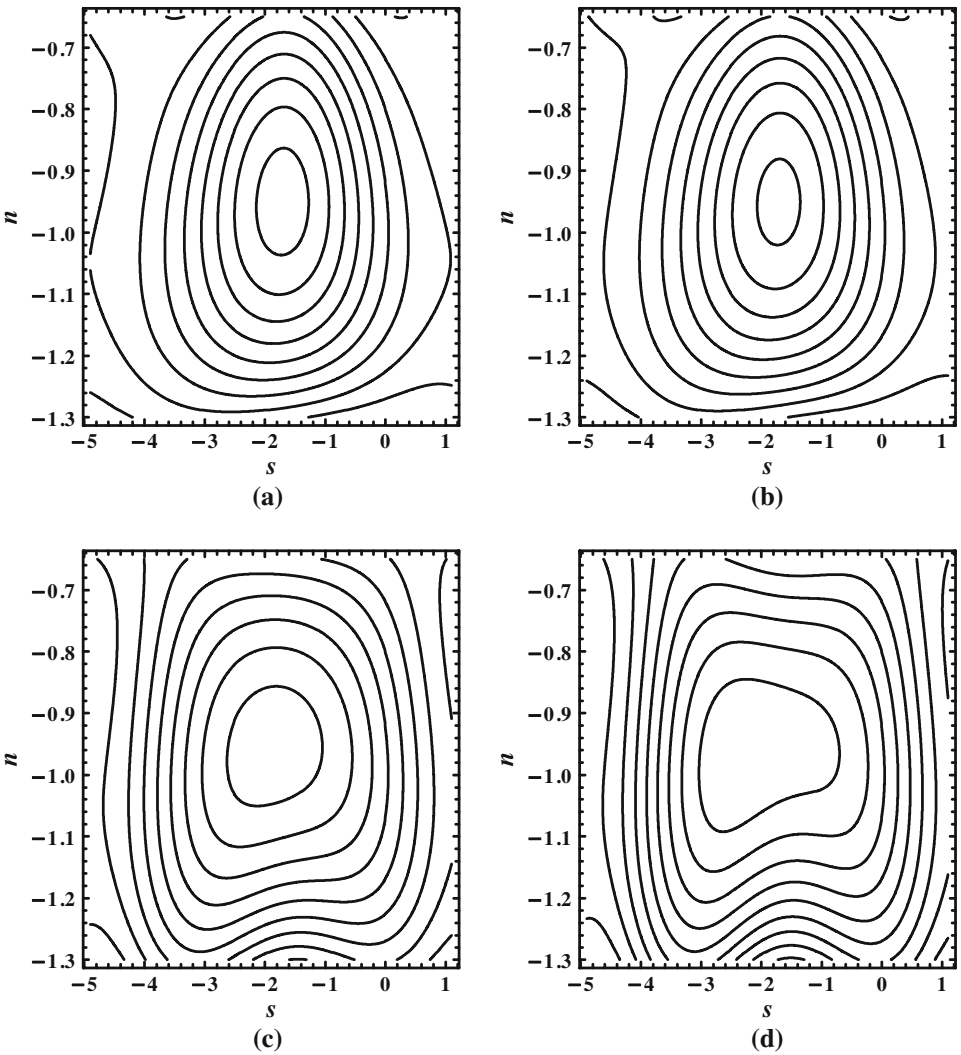

Fig. 17 Here the streamlines are plotted for against different values of W_e, i.e. **a** $W_e = 0.001$, **b** $W_e = 0.01$, **c** $W_e = 0.1$, **d** $W_e = 0.15$ while $B_r = 0.3, G_r = 0.2, k = 0.5, t = 0.05, \varepsilon = 0.05, E_1 = 1, E_2 = 5, E_3 = 1, E_4 = 5, E_5 = 1$ and $F = 2$

values of curvature parameter k. We note that with an increase in curve-ness of the channel the number of closed streamlines trapping boluses appearing in the left and right halves of the channel increases, for $k = 2$, i.e., small curve-ness, we note that the fluid flow pattern is quite similar to that of the fluid flow in a symmetric channel. For $k = 5$ we note that the size of the bolus increases as compared to (a). Figure 17 displays the streamlines for different values of W_e. We note that the orientation of the bolus varies with the variation of this parameter. For small value of W_e, i.e., $W_e = 0.001$ the bolus is oval shaped. When $W_e = 0.001$, we see that the bolus size shrinks and the shape of the streamlines enclosing the bolus becomes more oval. For $W_e = 0.1$, the W_e contributes in changing the orientation of the closed streamlines. For $W_e = 0.1$, we see that the shape of the bolus changes from oval to round. Figure 18 shows the streamlines for different values of B_r, the bolus grows with an increase in B_r. Moreover, the number of closed streamlines trapping the bolus increases. Figure 19 shows the streamlines for different values of G_r, the size of the bolus increases with an increase in G_r.

Conclusion

Here, we have examined the peristaltic flow of Williamson nanofluid in a curved channel comprising compliant walls. Key points are summarized as follows:

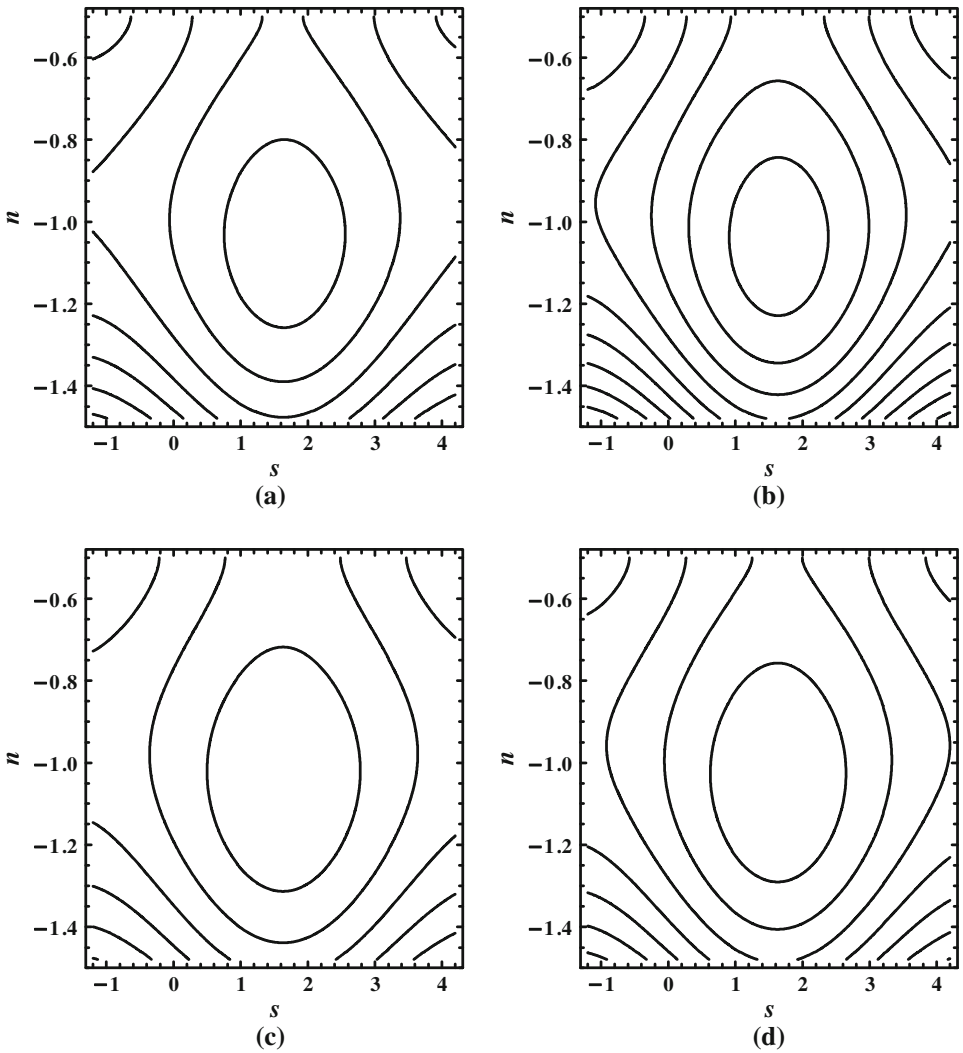

Fig. 18 Here the streamlines are plotted for against different values of B_r, i.e. **a** $B_r = 0.1$, **b** $B_r = 0.2$, **c** $B_r = 0.3$, **d** $B_r = 0.4$ while $G_r = 0.2$, $k = 0.5, W_e = 0.01, t = 0.05$, $\varepsilon = 0.05, E_1 = 0.1, E_2 = 0.5, E_3 = 0.1, E_4 = 0.5, E_5 = 0.1$ and $F = 2$

1. It is predicted that the fluid velocity increases with enhancing wall properties.
2. It is observed that in the inner half of the channel the increase in curve-ness contributes in reducing fluid velocity.
3. We note that the velocity increases with the increase in W_e in the region close to the inner wall and decreases in the region close to the outer wall of the curved channel.
4. It is noticed that with a rise in B_r, velocity increases.
5. It is seen that in the region close to the inner wall this increase is lessened as compared to the increase in the region close to the outer wall of the channel.
6. It is observed that an increase in the curvature parameter reduces temperature in the lower half of the channel while it contributes in raising temperature in the upper half of the channel.
7. We note that σ increases with the increase in k near the inner wall of the channel, but it decreases in the region beyond the inner wall to the outer wall region.
8. We note that with an increase in the curve-ness of the channel the number of closed streamlines trapping boluses appearing in the left and right halves of the channel increases, for $k = 2$, i.e., small curve-ness, we note that the fluid flow pattern is quite similar to that of the fluid flow in a symmetric channel.

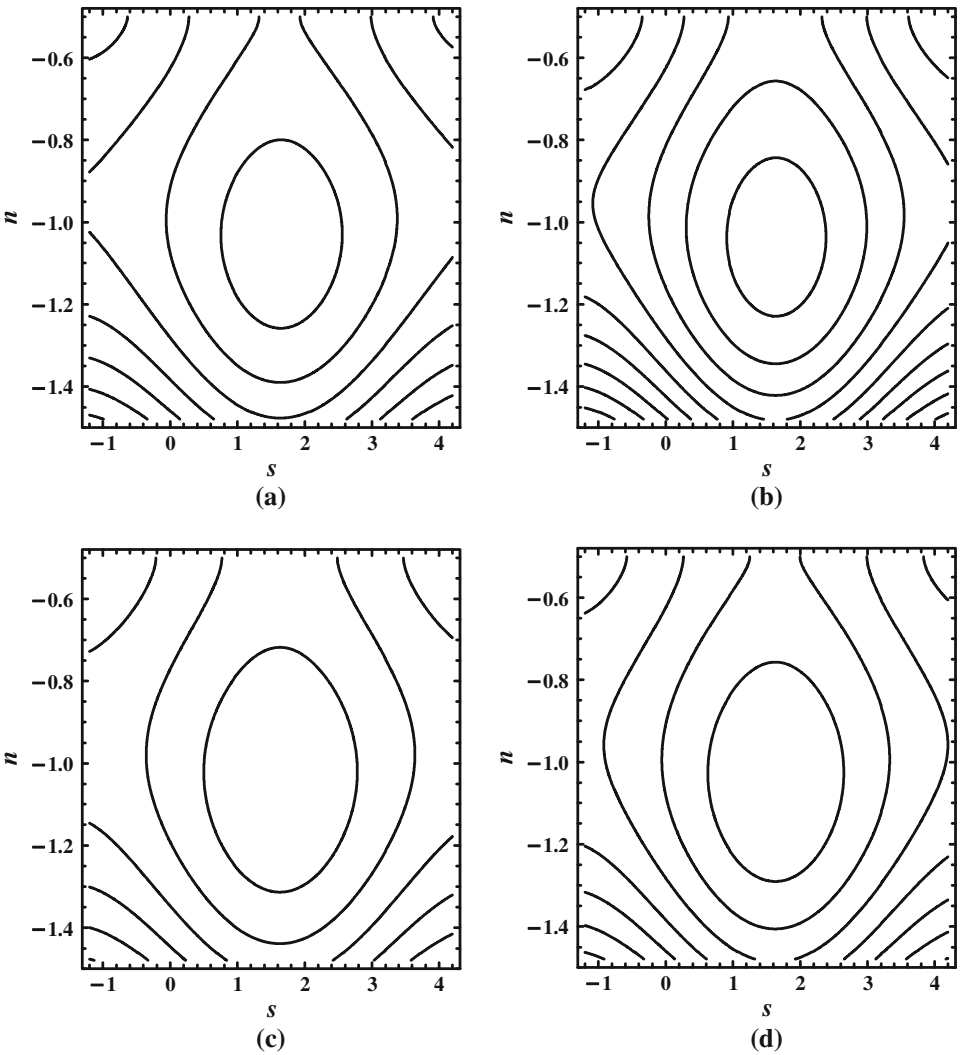

Fig. 19 Here the streamlines are plotted for against different values of G_r, i.e. **a** $G_r = 0.1$, **b** $G_r = 0.2$, **c** $G_r = 0.3$, **d** $G_r = 0.4$ while $B_r = 0.2, k = 0.5, W_e = 0.1, t = 0.05, \varepsilon = 0.05, E_1 = 0.1, E_2 = 0.5, E_3 = 0.1, E_4 = 0.5, E_5 = 0.1$ and $F = 2$

References

Afifi NAS, Mahmoud SR, Al-Isede HM (2011) Effect of magnetic field and wall properties on peristaltic motion of micropolar fluid. Int Math Forum 6:1345–1356

Akbar NS, Nadeem S (2011) Endoscopic effects on the peristaltic flow of a nanofluid. Commun Theor Phys 56:761–768

Akbar NS, Nadeem S (2012a) Thermal and velocity slip effects on the peristaltic flow of a six constant Jeffrey's fluid model. Int J Heat Mass Transf 55:3964–3970

Akbar NS, Nadeem S (2012b) Peristaltic flow of a Phan-Thien-Tanner nanofluid in a diverging tube. Heat Transf Res 41:10–22

Aziz A, Khan WA (2012) Natural convective boundary layer flow of a nanofluid past a convectively heated vertical plate. Int J Therm Sci 52:83–90

Choi SUS (1995) Enhancing thermal conductivity of fluids with nanoparticles. In: Siginer DA, Wang HP (eds) Developments and applications of non-newtonian flows, vol 66. ASME, New York, pp 99–105

Kramer MO (1960) Readers forum. J Aerosp Sci 68:27

Latham TW (1966) Fluid motion in a peristaltic pump. MS thesis, Massachusetts Institute of Technology, Cambridge

Marga SEB, Palm SJ, Nguyen CT, Roy G, Galanis N (2005) Heat transfer enhancement by using nanofluids in forced convection flows. Int J Heat Fluid Flow 26:530–546

Mekheimer KhS (2003) Nonlinear peristaltic transport through a porous medium in an inclined planar channel. J Porous Media 6:78

Mekheimer SKh, Abd elmaboud Y (2008) Influence of heat transfer and magnetic field on peristaltic transport of a Newtonian fluid in a vertical annulus. Application of an endoscope. Phys Lett A 372:1657–1665

Mittra TK, Prasad SN (1973) On the influence of wall properties and Poiseuille flow in peristalsis. J Biomech 6:681–693

Muthu P, Rathish Kumar BV, Chandra P (2001) Peristaltic motion in circular cylindrical tubes: effect of wall properties. Indian J Pure Appl Math 32(9):1317–1328

Muthu P, Rathish Kumar BV, Chandra P (2003) On the influence of wall properties in the peristaltic motion of micropolar fluid. ANZIAM J 45:245–260

Nadeem S, Akram S (2010) Peristaltic flow of a Williamson fluid in an asymmetric channel. Commun Nonlinear Sci Numer Simul 15:1705–1716

Nadeem S, Maraj EN (2012) The mathematical analysis for peristaltic flow of nano fluid in a curved channel with compliant walls. Appl Nanosci. doi:10.1007/s.13204.012.0165x

Radhakrishnamacharya G, Srinivasulu Ch (1999) Effect of elasticity of wall on peristaltic transport. In: Proceedings of ISTAM, India, pp 50–59

Radhakrishnamacharya G, Srinivasulu Ch (2007) Influence of wall properties on peristaltic transport with heat transfer. CR Mech 335:369–373

Rathod VP, Pallavi K (2011) The influence of wall properties on MHD peristaltic transport of dusty fluid. Adv Appl Sci Res 2(3):265–279

Saleh H, Roslan R, Hashima I (2011) Natural convection heat transfer in a nanofluid-filled trapezoidal enclosure. Int J Heat Mass Transf 54:194–201

Sato H, Kawai T, Fujita T, Okabe M (2000) Two dimensional peristaltic flow in curved channels. Trans Jpn Soc Mech Eng B 66:679–685

Srinivas S, Gayathri R (2009) Peristaltic transport of a Newtonian fluid in a vertical asymmetric channel with heat transfer and porous medium. Appl Math Comput 215:185–196

Srinivas S, Kothandapani M (2009) The influence of heat and mass transfer on MHD peristaltic flow through a porous space with compliant walls. Appl Math Comput 213:197–208

Srinivas S, Gayathri R, Kothandapani M (2009) The influence of slip conditions, wall properties and heat transfer on MHD peristaltic transport. Comput Phys Commun 180:2115–2122

Tripathi D, Pandey SK, Das S (2010) Peristaltic flow of viscoelastic fluid with fractional Maxwell model through a channel. Appl Math Comput 215:3645–3654